Neuropsychologia 184 (2023) 108561

Contents lists available at ScienceDirect

Neuropsychologia

journal homepage: www.elsevier.com/locate/neuropsychologia

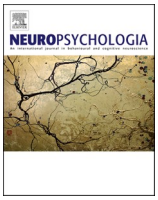

A transcranial magnetic stimulation study on the role of the left intraparietal sulcus in temporal orienting of attention

Mariagrazia Capizzi [a,b,*], Mar Martín-Signes [a,b], Jennifer T. Coull [c], Ana B. Chica [a,b,1], Pom Charras [d,1]

[a] Mind, Brain and Behavior Research Center (CIMCYC), University of Granada, Spain
[b] Department of Experimental Psychology, University of Granada, Spain
[c] Laboratoire de Neurosciences Cognitives UMR 7291, Aix-Marseille University, CNRS, Marseille, France
[d] Univ Paul Valéry Montpellier 3, EPSYLON EA 4556, F34000, Montpellier, France

ARTICLE INFO

Keywords:
Endogenous attention
Time
Foreperiod
Diffusion-weighted imaging
Superior longitudinal fasciculus

ABSTRACT

Adaptive behavior requires the ability to orient attention to the moment in time at which a relevant event is likely to occur. Temporal orienting of attention has been consistently associated with activation of the left intraparietal sulcus (IPS) in prior fMRI studies. However, a direct test of its causal involvement in temporal orienting is still lacking. The present study tackled this issue by transiently perturbing left IPS activity with either online (Experiment 1) or offline (Experiment 2) transcranial magnetic stimulation (TMS). In both experiments, participants performed a temporal orienting task, alternating between blocks in which a temporal cue predicted when a subsequent target would appear and blocks in which a neutral cue provided no information about target timing. In Experiment 1 we used an online TMS protocol, aiming to interfere specifically with cue-related temporal processes, whereas in Experiment 2 we employed an offline protocol whereby participants performed the temporal orienting task before and after receiving TMS. The right IPS and/or the vertex were stimulated as active control regions. While results replicated the canonical pattern of temporal orienting effects on reaction time, with faster responses for temporal than neutral trials, these effects were not modulated by TMS over the left IPS (as compared to the right IPS and/or vertex regions) regardless of the online or offline protocol used. Overall, these findings challenge the causal role of the left IPS in temporal orienting of attention inviting further research on its underlying neural substrates.

1. Introduction

Our interaction with the environment largely depends upon the ability to prioritize and selectively attend to relevant, rather than irrelevant, information. Although most studies of selective attention have focused on the spatial domain (e.g., Chica et al., 2013; Keefe and Störmer, 2021; Kuhns et al., 2017), there has also been an increase in research on the ability to selectively orient attention to *when* an event will occur, i.e., temporal orienting of attention (e.g., Capizzi et al., 2013; Coull and Nobre, 1998; Mento and Tarantino, 2015; Nobre and van Ede, 2018; Rohenkohl et al., 2014; Yeshurun and Tkacz-Domb, 2021).

One of the most widely used tasks to investigate temporal orienting of attention is the temporal orienting task, adapted from Posner's spatial orienting paradigm (Posner, 1980). In a typical implementation of the temporal orienting task (Coull and Nobre, 1998; Kingstone, 1992), each target presentation is preceded by a symbolic cue that indicates one of the two moments in time (early or late) that a target is likely to appear (though note that more than two time intervals can be cued; e.g., Coull et al., 2016). Cues can convey either correct (valid condition) or incorrect information (invalid condition) about the timing of target occurrence, or else they can provide no predictive information with trials equally divided between early and late cue-target intervals (neutral condition). The common finding is that reaction times (RTs) get faster and accuracy is higher for valid as compared to invalid or neutral trials, the so-called "temporal orienting effects" (Capizzi et al., 2012; Correa et al., 2004; Miniussi et al., 1999; Nobre, 2010). Temporal orienting effects are usually restricted to targets appearing at the shorter of the two time intervals, whereas they are reduced or even absent at the

* Corresponding author. Mind, Brain and Behavior Research Center (CIMCYC), University of Granada, Spain.
E-mail address: mgcapizzi@ugr.es (M. Capizzi).
[1] Joint senior author.

https://doi.org/10.1016/j.neuropsychologia.2023.108561
Received 3 November 2022; Received in revised form 21 February 2023; Accepted 5 April 2023
Available online 7 April 2023

longer interval. The lack of a behavioral benefit at longer time intervals is usually explained by the hazard function, i.e., the conditional probability that an event will occur given that it has not yet occurred (Herbst et al., 2018; Janssen and Shadlen, 2005; Visalli et al., 2019, 2021). That is, once a target that was cued to appear at the early interval fails to materialize, participants simply re-orient their attention to the longer time interval. Because of the hazard function, a behavioral advantage is also observed at long compared to short interval neutral trials, the so-called "foreperiod effect" (from the time interval between the cue and the target commonly termed the foreperiod; Capizzi and Correa, 2018; Niemi and Näätänen, 1981).

Performance on the temporal orienting task has been associated with activity in a variety of neural regions. Amongst these, functional magnetic resonance imaging (fMRI) studies especially point to the left intraparietal sulcus (IPS) as a key substrate for temporal orienting of attention (Bolger et al., 2014; Cotti et al., 2011; Coull and Nobre, 1998; Coull et al., 2016; Davranche et al., 2011). Indeed, significant activation of the left IPS in temporal orienting tasks has been reported independently of task demands (i.e., motor vs. perceptual; Davranche et al., 2011), type of responses (i.e., manual vs. saccadic; Cotti et al., 2011), or type of cues employed to direct attention to time (i.e., rhythms vs. symbolic cues; Bolger et al., 2014). However, the contribution of the left IPS to temporal orienting of attention is so far limited to correlational fMRI findings.

In the present study, we aimed to probe the causal role of the left IPS in temporal orienting of attention by perturbing its activity with transcranial magnetic stimulation (TMS). If left IPS plays a causal role in the ability to orient attention in time, we would expect the behavioral benefits of temporal orienting to be modulated following TMS over left IPS as compared to TMS over a control region (i.e., right IPS and vertex in Experiment 1; vertex in Experiment 2). No TMS modulation should be observed if left IPS activity is not causally related to temporal orienting.

In addition to TMS, we also acquired Diffusion-Weighted Imaging (DWI) data in order to explore the contribution of white matter connections between frontal and parietal areas to temporal orienting. Besides the parietal cortex, frontal regions have also been involved in temporal orienting of attention (Triviño et al., 2010, 2011). To our knowledge, no previous study has used DWI to explore whether white matter connections between frontal and parietal areas contribute to temporal orienting. To this end, we performed tractography of the Superior Longitudinal Fasciculus (SLF), an extensive longitudinal white matter tract connecting the frontal and parietal lobes. The SLF is composed of three different branches, labeled from dorsal to ventral: the SLF I (extending between the superior parietal lobe and the dorsal and medial parts of the frontal lobe), the SLF II (connecting the angular gyrus and the posterior regions of the superior and middle frontal gyrus), and the SLF III (extending between the supramarginal gyrus and the inferior frontal gyrus; Nakajima et al., 2019; Rojkova et al., 2016; Thiebaut de Schotten et al., 2011). The SLF has been linked to different attentional functions such as spatial orienting, sustained attention, and executive control in both healthy (Carretie et al., 2012; Klarborg et al., 2013; Sasson et al., 2012, 2013; Thiebaut de Schotten et al., 2011) and pathological populations with attentional deficits (e.g., spatial neglect: Doricchi et al., 2008; Thiebaut De Schotten et al., 2014; attention-deficit/hyperactivity disorder: Chiang et al., 2016; Wolfers et al., 2015). If the SLF also contributes to temporal orienting of attention, we would expect a significant correlation between the microstructural properties of this tract and temporal orienting effects.

2. Experiment 1

In Experiment 1, online repetitive TMS over left IPS, right IPS, and vertex was delivered while participants performed a temporal orienting task. Left IPS coordinates (see below) were extracted from a previous fMRI study showing greater activity in this area for temporally valid compared to neutral trials in both motor and perceptual temporal orienting tasks (Davranche et al., 2011). As control regions, both the right IPS and the vertex were stimulated. Right IPS coordinates were based on a TMS study providing evidence for the causal involvement of the right IPS in spatial orienting of attention (Chica et al., 2011). Considering that there was no spatial uncertainty in our temporal orienting task (as cue and target stimuli were both centrally displayed), we reasoned that stimulation of the left, but not right, IPS should selectively interfere with the ability to orient attention in time. Moreover, by stimulating the right IPS, we aimed to ensure that any potential interference by TMS on temporal orienting effects was specific to the left IPS only. As an additional control site, we stimulated the vertex because of previous reports showing no TMS modulation over the vertex on behavioral responses (Jung et al., 2016). TMS pulses were delivered immediately after the cue offset in order to selectively interfere with cue-induced temporal orienting processes (Davranche et al., 2011).

3. Methods

3.1. Participants

Twenty-two participants from the University of Granada took part in Experiment 1. Data from one participant were excluded because of poor compliance with task instructions (i.e., 9.16% of missed/anticipated responses), leaving a final sample size of twenty-one participants (12 females, mean age = 22.84 years, age range: 19–29 years), which is similar to the sample size of previous TMS studies from our group (Chica et al., 2011; Martín-Arévalo et al., 2019). A sensitivity power analysis (G*Power 3 software; Faul et al., 2007) showed that our sample size was adequate to detect significant ($\alpha = 0.05$) mean differences (one-tailed) between two dependent means (i.e., temporal orienting effects between left IPS and control region) with a medium effect size $d = 0.56$ and a statistical power of 0.80.

All participants reported to be right-handed, had normal or corrected-to-normal vision, and received monetary compensation for their participation (10 Euros/hour). All of them signed an informed consent prior to participation and completed security protocols for both MRI and TMS (Rossi et al., 2021). None of them reported a history of neurological or psychiatric disorders. The study was approved by the Ethics Committee of the University of Granada and was conducted in accordance with the recommendations of the Declaration of Helsinki.

3.2. Apparatus and stimuli

The experiment was run on an Intel® Core™ i5-64002 Duo personal computer connected to a 19″ LCD monitor (Benq T903, 1280 × 1024, 60 Hz). Stimulus presentation and data recording were controlled by E-prime software (Schneider et al., 2002). The viewing distance was approximately 60 cm. All stimuli were white, presented on a black background in the center of the screen (Fig. 1A). Stimuli were similar to those used in previous temporal orienting studies (Coull et al., 2013, 2016). They included a central stimulus (size: 1.91° × 1.91° of visual angle) comprising three concentric circles that served to create temporal and neutral cues, and a target. The temporal cues were associated with the brightening of the smallest (inner) and largest (outer) circle. The neutral cue was associated with the brightening of all the three circles. The target consisted of the presentation of a cross overlaid on the three circles.

3.3. Task and procedure

Fig. 1A illustrates the timing and the sequence of events forming a trial. Each trial started with the presentation of a blank screen for a random duration ranging from 500 to 1500 ms. The cue was then displayed for 500 ms. In the temporal condition, the brightening of the inner circle indicated that the target would appear after the short foreperiod (300 ms), whereas the brightening of the outer circle was

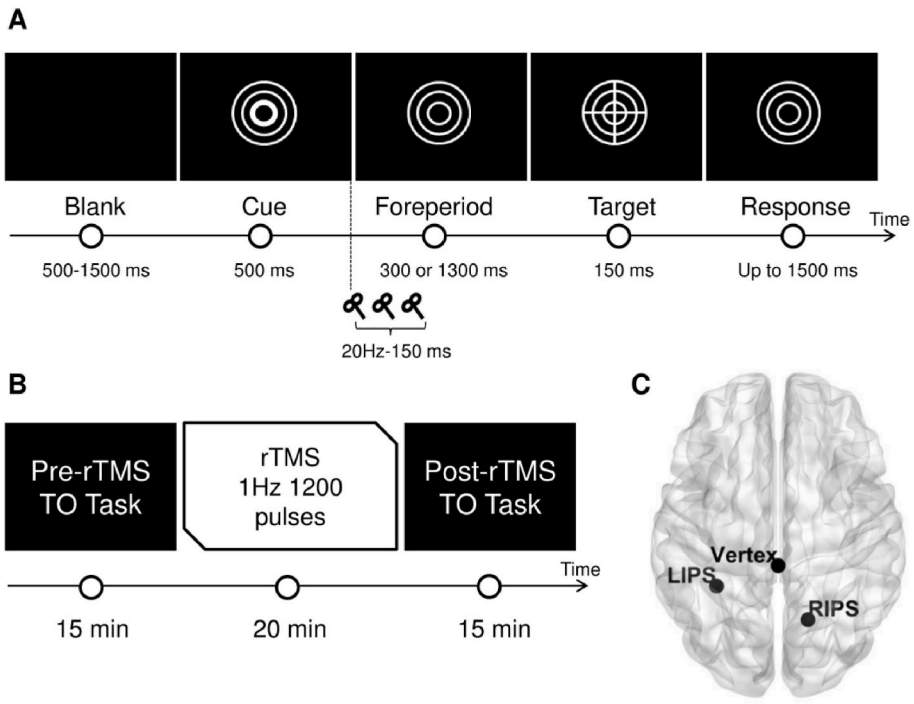

Fig. 1. (A). Schematic of the temporal orienting task used in Experiments 1 and 2. In Experiment 1, three TMS pulses were applied immediately after cue offset. **(B)** Illustration of the offline repetitive TMS (rTMS) protocol used in Experiment 2. Participants performed the temporal orienting task before and after receiving rTMS. **(C)** Representation of the TMS sites for Experiment 1 (LIPS, RIPS, and Vertex) in an axial brain view (Xia et al., 2013). In Experiment 2, only LIPS and Vertex were stimulated.

associated with the long foreperiod (1300 ms). Temporal cues were 100% valid. Participants were explicitly informed about cue validity and instructed to use the temporal cues to anticipate target onset. In the neutral condition, all three circles brightened meaning that the target was equally likely to appear after the short or the long foreperiod (50% probability for each foreperiod). At cue offset, the central stimulus comprising all three concentric circles was displayed for the entire foreperiod duration. After the foreperiod elapsed, the target (a cross overlaid on the three circles) appeared for 150 ms. Participants had to respond to the onset of the cross by pressing the left mouse button with their right hand as quickly as possible, while trying to avoid anticipations. A maximum of 1500 ms was allowed for responding. However, in case a response was initiated before target onset, a visual message, warning the participant to wait for the target, was displayed and the trial was repeated. After target response (or after 1500 ms for a missed response), there was an inter-trial-interval whose duration was adjusted on a trial-by-trial basis to never be less than 5 s. During the inter-trial-interval, the central circle comprising the three circles was presented.

For each stimulation site, there were 2 blocks of temporal cue trials and 2 blocks of neutral cue trials, each block containing 40 trials (equally divided into short and long foreperiods). Temporal and neutral blocks were alternated, and the condition with which participants started was counterbalanced. Before the experimental task, participants performed a training session comprising 12 neutral and 22 temporal trials to familiarize themselves with the meaning of the cues and the task.

3.4. MRI data acquisition

Structural images were collected on a 3-T Siemens Trio MRI scanner at the Mind, Brain, and Behavior Research Center (CIMCYC) of the University of Granada, using a 32 channel whole-head coil. High-resolution T1-weighted anatomical images (Repetition Time [TR] = 2530 ms, Echo Time [TE] = 3.5 ms, flip angle = 7°, slice thickness = 1 mm, field of view [FOV] = 256 mm) were collected. The DWI sequence consisted of 60 vol at *b*-value = 1500 s/mm^2 with gradient directions uniformly distributed in space and 6 vol at *b*-value = 0. For each volume, 70 near axial slices were acquired with a posterior–anterior phase of acquisition (TR = 8400 ms, TE = 88 ms, voxel size = 2 mm^3 isotropic, FOV = 220 mm, GRAPPA in plane acceleration factor = 3).

3.5. TMS procedure

The TMS session began by determining the hotspot for both the right and left first dorsal interosseous (FDI), the optimum site of the primary motor cortex (M1) evoking the highest contralateral motor evoked potentials (MEP) in the relaxed FDI. Then, we determined the right and left resting motor threshold (rMT), defined as the minimum stimulus intensity that elicits MEPs >50 mV in five out of ten consecutive trials (Rossini et al., 2015). Electromyography (EMG) and MEPs were recorded from left and right FDIs by using snap surface electrodes (Natus Neurology). During the experimental task, the stimulation was administered at 120% of each participant's rMT (averaging the rMT from the left and right FDI, and stimulating at a maximal intensity of 80% of the maximum stimulator output, MSO). Intensity of stimulation was decreased if participants presented any signs of discomfort such as blinks, yawn movements, etc. The mean stimulation intensity for the left IPS was 72.15 (*SD* = 8.15), whereas for the right IPS and vertex was 73.52 (*SD* = 8.27).

Participants received TMS over the left IPS [Montreal Neurological Institute (MNI) coordinates: x = −33, y = −45, z = 39, extracted from Davranche et al., 2011], the right IPS (MNI coordinates: x = 16, y = −63, z = 47, extracted from Chica et al., 2011), and the vertex (MNI = coordinates: x = 0, y = −34, z = 78, extracted from Martín-Arévalo et al., 2019) in counterbalanced order (Fig. 1C). Half of the participants started with the vertex stimulation, whereas the other half started with either the right or the left IPS stimulation. However, the blocks performed during the vertex stimulation (4 in total) were split in such a way that all participants received TMS over the vertex in between left and right IPS stimulations. For example, if one participant started with the left IPS stimulation, this was followed by vertex, right IPS and again vertex stimulation (i.e., LIPS/Vertex/RIPS/Vertex). Likewise, if one participant started with the vertex stimulation, then she/he underwent stimulation of the right (or the left) IPS followed by vertex stimulation (i.e., Vertex/RIPS/Vertex/LIPS). Trials from the vertex stimulations were collapsed for the analysis.

The stimulation consisted of three TMS pulses at 20 Hz (e.g., Fernández and Carrasco, 2020; Smith et al., 2005), delivered immediately after cue offset for a total duration of 150 ms. TMS was applied using a biphasic repetitive stimulator (Super Rapid 2, Magstim, Whitland UK) and a 70-mm TMS figure-of-eight refrigerated coil (Magstim, Whitland UK) positioned at ~45° respect to the scalp (e.g., Chanes et al., 2013; Chechlacz et al., 2015; Gallotto et al., 2022; Martín-Arévalo et al., 2019). The TMS coil was controlled by a robotic arm (TMS Robot; Axilum Robotics) and a TMS neuronavigation system (Brainsight; Rogue Systems, Montreal, Canada) with the capacity to estimate and track in real time the relative position, orientation, and tilting of the coil on the sectional and 3D reconstruction of the participants MRI with a precision of 5 mm (Caulfield et al., 2022).

3.6. Behavioral data analysis

Data from the practice session were discarded before any further analysis. Trials without responses and trials with premature responses (i.e., RTs <100 ms) were excluded (1.59% of all the trials). For each trial type (i.e., temporal-short, temporal-long, neutral-short, and neutral-long) at each stimulation site, RT values more extreme than one and a half times the interquartile range (i.e., the difference between the upper and lower quartile), above the upper quartile, or below the lower quartile were identified as outliers and removed from the analysis (5.41% of the remaining trials; Borcard et al., 2011; see also Vallesi et al., 2022, for a similar approach). Next, mean RTs were submitted to a repeated-measures ANOVA with Region (LIPS, RIPS, vertex), Condition (temporal, neutral) and Foreperiod (short, long) as within-participant factors. Significant interaction effects were followed up with paired dependent-sample *t*-tests. Partial Eta Squared (ηp^2) and Cohen's d (Cohen, 1977) were used as measures of effect size for ANOVAs and *t*-tests, respectively.

In addition to frequentist statistics, we also ran a Bayesian analysis in JASP (version 0.16.1 (JASP Team, 2022)) with the default JASP settings to calculate inclusion Bayes factors (BFs) for the repeated-measures ANOVA. Inclusion BFs quantify the evidence for including a specific main effect or interaction. A BF > 100 is regarded as extreme evidence, 30–100 very strong evidence, 10–30 strong evidence, 3–10 moderate evidence, 1–3 weak evidence and 1 no evidence (Wagenmakers et al., 2018). Inclusion BFs were obtained through Bayesian model averaging (across all models).

3.7. Diffusion weighted imaging (DWI) analysis

DWI data were pre-processed in ExploreDTI (Leemans and Jones, 2009) to attenuate artifacts commonly observed in diffusion MRI data. For each slice, DWI data were simultaneously registered and corrected for subject motion, and for eddy current and echo planar imaging distortions, adjusting the gradient accordingly (Irfanoglu et al., 2012; Leemans et al., 2009; Leemans and Jones, 2009). Spherical deconvolution was then performed employing the damped Richardson–Lucy deconvolution algorithm (Dell'Acqua et al., 2010) using StarTrack (http://www.natbrainlab.com). Algorithm parameters were $\alpha = 2$, algorithm iteration = 400, and $\eta = 0.06$ and $\nu = 8$ as regularization terms (Dell'Acqua et al., 2013). Whole-brain deterministic tractography was performed using a modified Euler tractography algorithm [angle threshold = 45°, absolute hindrance modulated (HMOA) threshold = 0.1, and relative threshold = 10%].

Individual dissections of the tracts were carried out with the software TrackVis (Wang et al., 2007). The 3 branches of the SLF (on the left and the right hemisphere) were isolated using a multiple region of interest (ROI) approach. Three frontal ROIs around the white matter of the superior, middle, and inferior frontal gyri, and a ROI around the white matter of the parietal lobe were delineated (see Rojkova et al., 2016; Thiebaut de Schotten et al., 2011, for a detailed explanation of the method). Streamlines of the arcuate fasciculus projecting to the temporal lobe were excluded by drawing a no-part ROI in the temporal white matter. Cingulate fibers were distinguished from the SLF I by delineating the frontal ROI above the cingulate sulcus. The HMOA, an index employed as a surrogate for tract microstructural organization, was extracted from each dissected tract. The mean HMOA is defined as the absolute amplitude of each lobe of the fiber orientation distribution; it is considered highly sensitive to axonal myelination, fiber diameter, and axonal density (Dell'Acqua et al., 2013).

We computed Pearson correlations between temporal orienting effects and the mean HMOA of the left and right SLF branches (SLF I, SLF II, and SLF III) separately. As a general measure of temporal orienting, we used the RT difference between temporal and neutral trials at the short foreperiod during the vertex stimulation. Both temporal orienting and SLF measures were normally distributed as assessed with Kolmogorov–Smirnov tests (all *ps* >. 2). Data from 19 participants were used for correlational analyses given that two participants did not complete DWI data acquisition. This and all the other correlation analyses reported here were corrected for multiple comparisons using a false discovery rate (FDR) correction ($p < .05$; Benjamini and Hochberg, 1995).

4. Results

As expected in a temporal orienting task,[2] the main effect of Condition was significant ($F(1, 20) = 23.72$, $p < .001$, $\eta_p^2 = .54$), with shorter RTs for temporal as compared to neutral trials. The main effect of Foreperiod was marginally significant ($F(1, 20) = 3.57$, $p = .073$, $\eta_p^2 = .15$), as it was better qualified by a significant Condition × Foreperiod interaction ($F(1, 20) = 36.33$, $p < .001$, $\eta_p^2 = .64$), such that RTs got faster at the long foreperiod as compared to the short foreperiod in the neutral condition only ($t_{(20)} = 4.74$, $p < .001$, $d = 1.03$). By contrast, in the temporal condition, RTs tended to be faster at the short foreperiod as compared to the long foreperiod ($t_{(20)} = 2.05$, $p = .054$, $d = 0.44$). More importantly, reflecting the classic temporal orienting effects, pairwise comparisons at each foreperiod showed that RTs were faster for temporal than neutral trials at the short foreperiod ($t_{(20)} = 5.82$, $p < .001$, $d = 1.27$), but RTs did not differ between temporal and neutral trials at the long foreperiod ($t_{(20)} = 1.26$, $p = .22$, $d = 0.27$). The main effect of Region and all interactions involving the Region Factor did not approach significance (minimum $p = .17$; Fig. 2).

Despite the lack of a significant Region x Condition × Foreperiod interaction in our data, we calculated for each stimulation site an index of temporal orienting (i.e., RT difference between temporal and neutral trials at the short foreperiod) and compared the magnitude of temporal orienting effects across stimulation sites with a one-way ANOVA with Region as factor. This analysis confirmed no difference in temporal orienting effects ($Mean_{LIPS} = 38.12$, $SD = 46.29$; $Mean_{RIPS} = 29.39$, $SD = 23.11$; $Mean_{Vertex} = 37.77$, $SD = 25.2$) between stimulation sites ($F(2, 60) = 0.46$, $p = .6$, $\eta_p^2 = .015$).

The results from the frequentist analysis were supported by Bayesian statistics showing that there was extreme evidence for including the main effects of Condition (inclusion BF = 4.569e+12), Foreperiod (inclusion BF = 312242.312), and their interaction (inclusion BF = 589757.580). Conversely, there was no evidence for including the main effect of Region (inclusion BF = 0.358) as well as all interactions involving the Region factor (inclusion BFs for Region x Condition = 0.090, Region x Foreperiod = 0.103, and Region x Condition x Foreperiod = 0.019).

As concerns the results from DWI tractography, temporal orienting effects were not correlated with the HMOA index of any of the left or

[2] Although our focus was on temporal orienting, the presence of a neutral condition granted us the possibility to explore the role of the left IPS in the expression of foreperiod effects and sequential effects (SEs; Capizzi et al., 2015; Los et al., 2014; Vallesi et al., 2013). The analysis on SEs can be found in the Supplementary material.

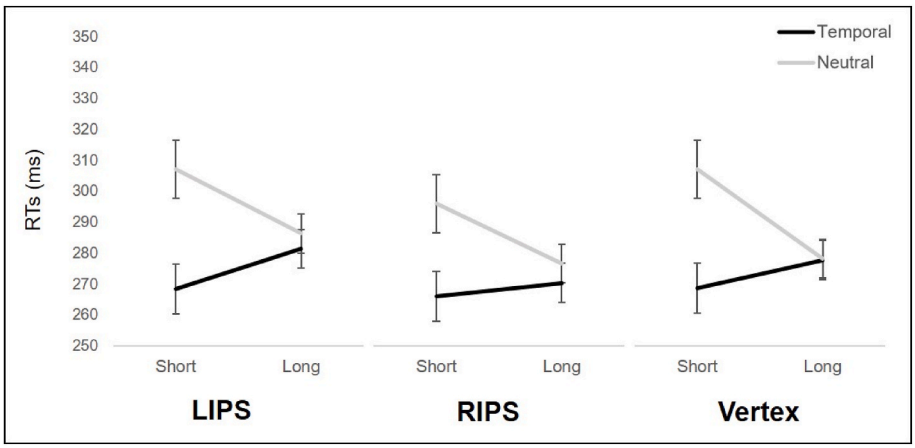

Fig. 2. Reaction time (RTs) results from Experiment 1. Mean RTs in milliseconds (ms) as a function of Region (LIPS, RIPS, and Vertex), Condition (temporal, neutral) and Foreperiod (short, long). Error bars represent standard error of the mean.

right SLF branches (minimum $p_{uncorr} = .16$).

5. Discussion

While our results replicated previous findings of temporal orienting effects, with significant benefits for temporal versus neutral trials at the short foreperiod (Capizzi et al., 2012; Correa et al., 2004; Coull and Nobre, 1998), these effects were not modulated by TMS over the left IPS. Specifically, participants showed comparable temporal orienting effects regardless of the stimulation site, either left or right IPS or vertex region. Moreover, Bayesian analysis confirmed that our data were best represented by a model including both Condition and Foreperiod factors and their interaction rather than a model that also included possible interactions with the Region factor.

The absence of an effect of left IPS stimulation on temporal orienting was unexpected in light of previous fMRI studies pointing to this region as a key substrate for orienting attention in time (Bolger et al., 2014; Cotti et al., 2011; Coull and Nobre, 1998; Coull et al., 2016; Davranche et al., 2011). Although there are multiple possibilities as to why stimulation did not elicit an effect (de Graaf and Sack, 2011), one explanation for this null finding relates to the use of an online TMS protocol. That is, one could argue that our online TMS approach, covering a short temporal range only (i.e., 150 ms), was perhaps inadequate to disrupt temporal orienting effects. Another related possibility is that the left IPS might only become involved at the moment at which the target is predicted to appear, rather than at the onset of the interval being timed. Delivering TMS at cue offset might therefore have spared attentional processes that are temporally focused on target onset. Experiment 2 aimed to test these possibilities by employing an offline TMS protocol. Offline stimulation would allow for a more stringent test of the contribution of the left IPS to temporal orienting by producing stronger effects that cover the entire trial. As in Experiment 1, DWI tractography of the SLF was performed.

6. Experiment 2

Experiment 2 was a replication of Experiment 1 with the critical exception that offline, instead of online, TMS was used. In particular, we devised a pre-post design, with a repetitive TMS (rTMS) sequence of 1200 pulses applied at 1 Hz. Because an offline TMS procedure involves at least two different sessions to stimulate both target and control region (s), in Experiment 2 we simplified the design by keeping only the vertex as a control site.

7. Methods

7.1. Participants

Twenty-two participants were recruited for Experiment 2. None of them had participated in Experiment 1. Three participants did not return to complete the second TMS session and were then replaced with other three participants. One participant was rejected because data from one session got lost. The final sample included 21 participants (13 females, mean age = 25.05 years, age range: 19–36 years, all right-handed according to self-report). As in Experiment 1, all participants completed security protocols for both MRI and TMS, signed an informed consent prior to the study, and received monetary compensation for their participation (10 Euros/hour).

7.2. Apparatus, stimuli and procedure

The apparatus, stimuli, and procedure were the same as in Experiment 1 with the exception that rTMS over left IPS and vertex were applied offline in two separate sessions on two different days (Fig. 1B). In each session, participants performed the same temporal orienting task as in Experiment 1. The task was divided into 4 blocks of 40 trials each, with two of the blocks comprising the temporal condition and two blocks the neutral condition. Participants performed this task twice in each session, once before (pre-rTMS) and once after (post-rTMS) TMS stimulation.

7.3. MRI data acquisition and DWI analysis

MRI data acquisition was the same as in Experiment 1 with the exception of the DWI sequence, which was optimized according to recent work (Guo et al., 2020; Jeurissen et al., 2014). We used a DWI multiband and multi-shell acquisition protocol (TR = 3500 ms, TE = 75 ms, voxel size = 1.8 mm^3 isotropic, FOV = 208 mm, multi-band acceleration factor = 3). We acquired, in consecutive sequences, 8 vol at b = 300 s/mm^2 (2 *b* value = 0 vol), 32 vol at b = 1000 s/mm^2 (6 *b* value = 0 vol), and 60 vol at b = 2000s/mm^2 (6 *b* value = 0 vol). For each volume, 81 near axial slices were collected with a posterior–anterior phase of acquisition. Additionally, the *b*-value 300 sequence was acquired with an anterior-posterior phase of acquisition to correct for phase-encoding direction-induced distortions (Andersson et al., 2003).

DWI data pre-processing was similar to that used in Experiment 1 using the *eddy* current correction tool from the FMRIB Software Library (FSL, Andersson and Sotiropoulos, 2016). Additionally, distortions induced by phase encoding were corrected using the *topup* toolbox from FSL (Andersson et al., 2003). Multishell spherical deconvolution (Guo

et al., 2020) was then performed with the algorithm parameters $\alpha = 2$, algorithm iteration = 400, and $\eta = 0.001$ and $\nu = 8$ as regularization terms. Whole-brain deterministic tractography was performed using a modified Euler tractography algorithm (angle threshold = 45° and HMOA threshold = 0.0036).

Dissections of the right and left SLF I, SLF II, and SLF III were performed as in Experiment 1. Likewise, Pearson correlations between temporal orienting effects and the mean HMOA of the left and right SLF branches were computed separately. Temporal orienting effects (i.e., RT difference between temporal and neutral trials at the short foreperiod) were calculated using data from the pre-TMS blocks only, collapsing across pre-left IPS and pre-vertex sessions. All the measures were normally distributed (all *ps* >. 20). Data from 18 participants contributed to the correlational analyses.

7.4. rTMS procedure

The first TMS session began by determining the participants' rMT. EMG and MEPs were recorded from the right FDI. During the experimental task, TMS was administered at 100% of each participant's rMT, decreasing the intensity of stimulation in the presence of blinks, yawn movements or any other signs of discomfort. Each participant underwent 2 TMS sessions, separated by at least five days (mean inter-session interval = 8 days, *SD* = 3.13). One participant returned for the second session after two months for medical reasons. Results did not change when excluding this participant. Half of the participants started with the left IPS stimulation (mean stimulation intensity = 63.95 of MSO, *SD* = 7.19), whereas the other half started with the vertex stimulation (mean stimulation intensity = 64.57, *SD* = 7.51). The rTMS sequence consisted of 1200 pulses applied at 1 Hz with an inter-pulse interval of 1 s (for a total duration of 20 min). Previous studies have shown that this protocol transiently reduces cortical excitability within the stimulated sites and lasts for approximately 50–75% of the stimulation duration (Chen et al., 1997; Maeda et al., 2000; Muellbacher et al., 2000; Hilgetag et al., 2001; Wagner et al., 2007), which should cover most of our post-rTMS task (15 min).

7.5. Behavioral data analysis

The same trimming procedure (1.84% rejected trials of all the trials) and RT outlier removal (6.3% of the remaining trials) as in Experiment 1 were applied. A repeated-measure ANOVA was used on mean RTs, with Region (LIPS, vertex), Session (pre-TMS, post-TMS), Condition (temporal, neutral), and Foreperiod (short, long) as within-participant factors.

8. Results

The ANOVA yielded significant effects of Condition ($F(1, 20) = 32.3$, $p < .001$, $\eta_p^2 = .62$), Foreperiod ($F(1, 20) = 18.3$, $p < .001$, $\eta_p^2 = .48$), and their interaction ($F(1, 20) = 40.3$, $p < .001$, $\eta_p^2 = .67$). Replicating Experiment 1,[3] post-hoc pairwise comparisons at each foreperiod showed significant temporal orienting effects (i.e., shorter RTs for temporal compared to neutral trials) at the short foreperiod ($t_{(20)} = 7.06$, $p < .001$, $d = 1.54$), but not at the long foreperiod ($t_{(20)} = 1.13$, $p = .27$, $d = 0.24$). The main effect of Session was also significant ($F(1, 20) = 27.4$, $p < .001$, $\eta_p^2 = .58$), indicating that participants responded faster in the post-TMS session as compared to the pre-TMS session.

The main effect of Region and all the interactions involving the Region factor failed to reach significance (minimum $p = .14$; Fig. 3), except for the Region x Session × Foreperiod interaction ($F(1, 20) = 4.38$, $p = .049$, $\eta_p^2 = .18$). In order to unpack this three-way interaction, we analyzed the Session × Foreperiod interaction separately for the left IPS and vertex. These follow-up analyses showed that the Session by Foreperiod interaction was not significant for the left IPS ($F < 1$), whereas it was marginally significant for the vertex region ($F(1, 20) = 4.15$ $p = .054$, $\eta_p^2 = .17$). Further unpacking this interaction for the vertex, the foreperiod effect was significant in the pre-TMS session ($t_{(20)} = 3.57$, $p = .002$, $d = 0.78$), but not in the post-TMS session ($t_{(20)} = 1.92$, $p = .068$, $d = 0.42$). Note, however, that the Region x Session × Foreperiod interaction was only supported by frequentist but not by Bayesian statistics (inclusion BF = 0.014), as detailed below.

As in Experiment 1, Bayesian statistics showed that there was extreme evidence for including the main effects of Condition (inclusion BF = 2.0229e+13), Foreperiod (inclusion BF = 1.824e+12), and their interaction (inclusion BF = 2.650e+7). Moreover, there was extreme evidence for including the main effect of Session (inclusion BF = 5.820e+6). By contrast, there was weak evidence for including the main effect of Region (inclusion BF = 2.065), and no evidence for including all the interactions involving the Region factor (inclusion BFs< 1).

Replicating Experiment 1, temporal orienting effects were not correlated with any of the HMOA indexes of the left or right SLF branches (minimum $p_{uncorr} = .53$).

8.1. Post-hoc DWI tractography analysis

Recent studies suggest that TMS modulation of behavioral performance on attentional tasks may, in part, depend on the microstructural properties of white matter branches such as the SLF. In particular, larger TMS effects have been observed for participants with lower HMOA values as compared to participants with higher HMOA values in certain SLF fascicules (Martín-Signes et al., 2019, 2021). This suggests that high HMOA values in the SLF tract could counteract the disruptive consequences of TMS application. Building on this line of research, we explored whether white matter microstructural properties of the SLF might also have had a role in our null neuromodulation results. To this aim, we performed post-hoc correlational analyses between HMOA indexes of the left SLF branches and RT indices of the hypothesized interaction between region and temporal orienting effects, as in previous work from our group (see Martín-Signes et al., 2021). For Experiment 1, the interaction index was calculated by subtracting the temporal orienting effects (i.e., RT difference between temporal and neutral trials at the short foreperiod) for the left IPS TMS from the temporal orienting effects for the vertex TMS (i.e., the control region common to both experiments). For Experiment 2, since in addition to the comparison between regions (left IPS, vertex), there was also the comparison between sessions (pre, post), we simplified the analyses by calculating two separate indexes: one for the left IPS (i.e., pre(temporal-neutral) minus post(temporal-neutral) and one for the vertex (i.e., pre (temporal-neutral) minus post(temporal-neutral). Then, we correlated the obtained interaction indexes[4] with the left SLF branches. Neither of these correlations was significant (minimum $p_{uncorr} = .12$).

9. Discussion

Experiment 2 again provided no evidence for a modulation of temporal orienting effects by TMS over the left IPS. This result showed that interfering with left IPS activity even with an offline TMS protocol was insufficient to disrupt the ability to voluntarily orient attention in time.

10. General discussion

This study investigated for the first time the causal role of the left IPS in temporal orienting of attention. Participants performed a classic

[3] As for Experiment 1, the analysis on SEs is reported in the Supplementary material.

[4] Note that it was not possible to derive a single index collapsing the data from both experiments because DWI sequences differed between the two acquisition protocols.

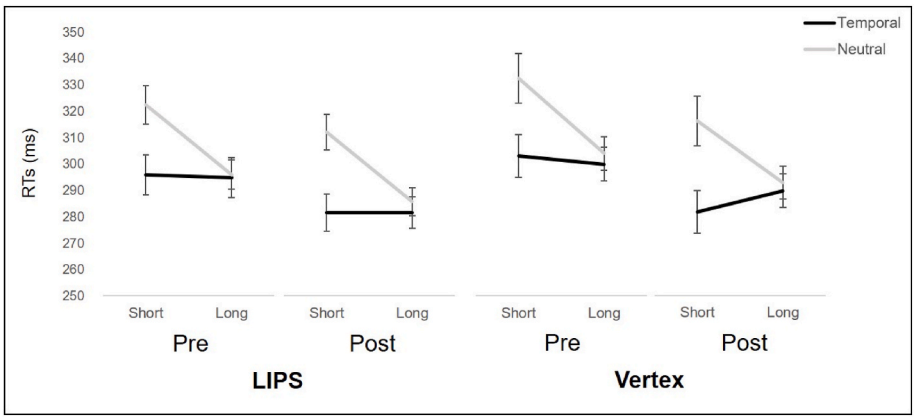

Fig. 3. Reaction time (RTs) results from Experiment 2. Mean RTs in milliseconds (ms) as a function of Region (LIPS, Vertex), Session (pre, post), Condition (temporal, neutral) and Foreperiod (short, long). Error bars represent standard error of the mean.

temporal orienting task with two foreperiods randomized on a trial-by-trial basis. Valid temporal blocks, affording anticipatory preparation, were alternated with neutral blocks in which the cue did not convey any predictive information about the timing of target onset. Experiment 1 tested the hypothesis that selectively interfering with left IPS activity during the cue period should lead to reduced temporal orienting effects as compared to TMS over either the right IPS or the vertex region. Experiment 2 employed an identical temporal orienting task as in Experiment 1, but with an offline stimulation protocol aimed to increase TMS-induced interference effects by covering the entire trial.

Findings from both experiments replicated the typical pattern of temporal orienting effects, with shorter RTs for temporal than neutral trials at the short foreperiod. Moreover, we also corroborated the well-known advantage afforded by the passage of time (i.e., foreperiod effect) and the duration of the preceding foreperiod (i.e., sequential effects; see the Supplementary Material). Overall, these results confirm the reliability of our task manipulation, discounting the possibility that null TMS effects reflected a problem in the experimental design. The null results might instead reflect a problem with the TMS protocol. However, several arguments help dispute this possibility, thereby strengthening the meaningfulness and interpretability of our negative TMS findings. As outlined in de Graaf and Sack (2011), these arguments are: the "localization" argument, the "neural efficacy" argument, and the "power" argument.

The *localization argument* concerns the extent to which the targeted cortical region was actually stimulated with TMS. Regarding our study, the co-registration of coil placement with individual MRI images and the use of a real-time neuro-navigation system ensured precise anatomical targeting. It is, thus, very likely that the desired left IPS coordinates were successfully stimulated in our experiments. Nevertheless, IPS morphology is highly variable across individuals (Zlatkina and Petrides, 2014). The anatomical location of an x,y,z coordinate in one participant may not be exactly the same as that in another participant, and such individual differences may be even greater for points deep (~2 cm) within the sulcus (such as that targeted in the current study). One might indeed wonder whether this point laid outside the stimulation range of our coil, although previous studies from our lab have successfully targeted regions that are equally deep (Bourgeois et., 2013; Chica et al., 2011; Ortiz-Tudela et al., 2018). Finally, the stereotaxic coordinates associated with temporal orienting varies quite widely from one fMRI study to the next, covering an area from a relatively medial point deep within the IPS out towards more lateral regions of the cortical surface (Coull, 2015). Therefore, before concluding that TMS of the parietal lobe has no effect on temporal orienting, it would be wise to repeat this experiment with stimulation of another, more lateralized, region of inferior parietal cortex and/or one that is closer to the surface.

The *neural efficacy* argument posits that, even if the intended brain region was properly targeted, perhaps the selected TMS protocol was inadequate to interfere with its activity. This argument can be countered as we employed two established TMS protocols associated with robust behavioral effects, and neither of the two protocols modulated temporal orienting. Moreover, even if it could be argued that online TMS failed to interfere with left IPS-dependent processes manifest at the target, rather than cue, stage of the task, this explanation does not hold for the offline stimulation of Experiment 2, which covered the entire trial. Finally, even though we admit that significant TMS effects on a control task would have reinforced the neural efficacy of our TMS protocols (de Graaf and Sack, 2018), it is worth mentioning that protocols similar to those used here have successfully modulated spatial orienting processes in prior work from our group (e.g., Bourgeois et al., 2013; Chica et al., 2014). This constitutes indirect evidence that our TMS protocols can modulate attentional orienting in Posner-like paradigms, thus mitigating a criticism related to the neural efficacy argument. A further control in future research would be to measure brain activity with fMRI before and after TMS to check for stimulation-dependent effects on the activation or coactivation of the targeted brain region with other regions of the attentional network (e.g., Orpella et al., 2020). Moreover, considering that coil orientation may also affect current flow direction (e.g., Gomez-Tames et al., 2018; Laakso et al., 2014), it would be also interesting to explore whether a coil orientation different than the 45° used here (e.g. 10° inducing a posterior-anterior flow; Koch et al., 2008) might have a role in the efficiency of TMS. As last point, with respect to the *power argument*, it is unlikely that this was an issue in our study as both frequentist and Bayesian statistics converged on the conclusion that there was no significant TMS modulation. In any case, bigger sample sizes are warranted in future studies to further analyze the impact of TMS on temporal orienting of attention.

Based on the above, our null TMS findings provide initial evidence that disruption of the left IPS is insufficient to perturb the ability to orient attention in time. Provided however that there are no similar TMS studies targeting left IPS activity in temporal orienting, caution is warranted when speculating on the absence of TMS effects over left IPS. The most likely explanation is that the left IPS is, in fact, engaged during the temporal orienting task, as shown in fMRI studies, but that this is not the only region necessary for the successful deployment of temporal attention, which would instead rely on the functioning of a distributed neural network (Coull et al., 2013). This explanation is consistent with neuropsychological (Triviño et al., 2010, 2011, 2016) and neuroimaging (Coull and Nobre, 1998; Coull et al., 2001, 2008, 2013) observations that regions anatomically connected to the parietal cortex, such as premotor and frontal regions, are also important for temporal orienting. Supporting this, Correa et al. (2014) provided evidence for an effect of TMS over right and left dorsolateral prefrontal cortex (vs. sham) on temporal orienting effects (i.e., increased benefits due to reduced RTs on

valid trials). More recently, a set of neuropsychological studies has also highlighted the contribution of the cerebellum to temporal orienting (Breska and Ivry, 2018, 2020, 2021), confirming previous neuroimaging results (Coull and Nobre, 1998; Coull et al., 2013), and bringing to the forefront the, yet underestimated, role of subcortical regions in the ability to orient attention in time. Under the scenario of a widespread network encompassing both cortical and subcortical areas in temporal orienting of attention, it is possible that disruption of a single node of this network, like the left IPS, could have been compensated for by activity in other brain regions. Of course, this hypothesis requires further non-invasive brain stimulation investigation as, for the moment, it remains speculative.

The following findings deserve some final consideration. As introduced earlier, our study also tested for white matter contributions to temporal orienting by analyzing DWI data. Specifically, we focused on the superior longitudinal fasciculus (SLF), on the premise that this white matter tract has already been associated with spatial attentional processes (Carretie et al., 2012; Thiebaut de Schotten et al., 2011). With the proper caution, considering the explorative nature of these correlational analyses and the small sample size of our study, results showed no significant association between the SLF and temporal orienting ability. Moreover, unlike previous studies from our group (Martín-Signes et al., 2019, 2021), we did not find evidence that individual variability in neuromodulation effects could be explained by white matter properties. Future studies are needed to corroborate these preliminary findings, which indirectly hint at differences in the white matter properties related to spatial and temporal orienting of attention.

To conclude, the present study challenges the causal role of the left IPS in temporal orienting of attention, suggesting that such a fundamental cognitive ability is likely mediated by a widespread network, not limited to the activity of the left IPS.

Author contributions

A.B.C., J.T.C. and P.C. designed research; **M.C., A.B.C., and P.C.** performed research; **M.C. and M.M-S.** analyzed data; **M.C.** wrote the first draft of the manuscript; **M.C., M.M-S, J.T.C., A.B.C., and P.C.** wrote, reviewed and edited the manuscript.

Data availability

Raw behavioral data and DTI values are publicly available via Open Science Framework (https://osf.io/kxmtw/).

Acknowledgments

This work was funded by an Agence National de Recherche grant (ANR-18-CE28-0009-01) to P.C. M.C. is supported by a grant (PID2021-128696NA-I00) funded by MCIN/AEI/10.13039/501100011033 and by "ERDF A way of making Europe", and by a María Zambrano Fellowship at the University of Granada from the Spanish Ministry of Universities and the European Union Next Generation. M.M-S. is supported by a "Margarita Salas" fellowship by the Spanish Ministry of Universities and the European Union Next Generation, and by a contract for Young Researchers (PAIDI 2020) by the Ministry of Economy, Knowledge, Enterprise, and Universities of Andalusia. A.B.C. is supported by the Spanish Ministry of Science and Innovation (PSI2017-88136 and PID2020-119033 GB-I00) and FEDER-Junta de Andalucía (A.SEJ.090. UGR18). Funding for open access charge: Universidad de Granada / CBUA.

Appendix A. Supplementary data

Supplementary data to this article can be found online at https://doi.org/10.1016/j.neuropsychologia.2023.108561.

References

Andersson, J.L., Skare, S., Ashburner, J., 2003. How to correct susceptibility distortions in spin-echo echo-planar images: application to diffusion tensor imaging. NeuroImage 20 (2), 870–888.
Andersson, J.L., Sotiropoulos, S.N., 2016. An integrated approach to correction for off-resonance effects and subject movement in diffusion MR imaging. NeuroImage 125, 1063–1078.
Benjamini, Y., Hochberg, Y., 1995. Controlling the false discovery rate: a practical and powerful approach to multiple testing. J. Roy. Stat. Soc. B 57, 289–300.
Bolger, D., Coull, J.T., Schön, D., 2014. Metrical rhythm implicitly orients attention in time as indexed by improved target detection and left inferior parietal activation. J. Cognit. Neurosci. 26 (3), 593–605.
Borcard, D., Gillet, F., Legendre, P., 2011. Numerical Ecology with R. Springer, New York.
Bourgeois, A., Chica, A.B., Valero-Cabre, A., Bartolomeo, P., 2013. Cortical control of inhibition of return: causal evidence for task-dependent modulations by dorsal and ventral parietal regions. Cortex 49 (8), 2229–2238.
Breska, A., Ivry, R.B., 2018. Double dissociation of single-interval and rhythmic temporal prediction in cerebellar degeneration and Parkinson's disease. Proc. Natl. Acad. Sci. USA 115 (48), 12283–12288.
Breska, A., Ivry, R.B., 2020. Context-specific control over the neural dynamics of temporal attention by the human cerebellum. Sci. Adv. 6 (49), eabb1141.
Breska, A., Ivry, R.B., 2021. The human cerebellum is essential for modulating perceptual sensitivity based on temporal expectations. Elife 10, e66743.
Capizzi, M., Correa, Á., 2018. Measuring temporal preparation. In: Vatakis, A., Balci, F., Di Luca, M., Correa, Á. (Eds.), Timing and Time Perception: Procedures, Measures, and Applications. Brill, Leiden Boston, pp. 216–232.
Capizzi, M., Correa, Á., Sanabria, D., 2013. Temporal orienting of attention is interfered by concurrent working memory updating. Neuropsychologia 51, 326–339.
Capizzi, M., Correa, Á., Wojtowicz, A., Rafal, R.D., 2015. Foreperiod priming in temporal preparation: testing current models of sequential effects. Cognition 134, 39–49.
Capizzi, M., Sanabria, D., Correa, Á., 2012. Dissociating controlled from automatic processing in temporal preparation. Cognition 123, 293–302.
Carretie, L., Rıos, M., Perianez, J.A., Kessel, D., Alvarez-Linera, J., 2012. The role of low and high spatial frequencies in exogenous attention to biologically salient stimuli. PLoS One 7 (5), 1–8.
Caulfield, K.A., Fleischmann, H.H., Cox, C.E., Wolf, J.P., George, M.S., McTeague, L.M., 2022. Neuronavigation maximizes accuracy and precision in TMS positioning: evidence from 11,230 distance, angle, and electric field modeling measurements. Brain Stimul. 15 (5), 1192–1205.
Chanes, L., Quentin, R., Tallon-Baudry, C., Valero-Cabré, A., 2013. Causal frequency-specific contributions of frontal spatiotemporal patterns induced by non-invasive neurostimulation to human visual performance. J. Neurosci. 33 (11), 5000–5005.
Chechlacz, M., Humphreys, G.W., Sotiropoulos, S.N., Kennard, C., Cazzoli, D., 2015. Structural organization of the corpus callosum predicts attentional shifts after continuous theta burst stimulation. J. Neurosci. 35 (46), 15353–15368.
Chen, R., Classen, J., Gerloff, C., Celnik, P., Wassermann, E.M., Hallett, M., Cohen, L.G., 1997. Depression of motor cortex excitability by low-frequency transcranial magnetic. Neurology 48, 1398–1403.
Chiang, H.-L., Chen, Y.-J., Shang, C.-Y., Tseng, W.-Y.I., Gau, S.S., 2016. Different neural substrates for executive functions in youths with ADHD: a diffusion spectrum imaging tractography study. Psychol. Med. 46 (6), 1225e1238.
Chica, A.B., Bartolomeo, P., Lupiáñez, J., 2013. Two cognitive and neural systems for endogenous and exogenous spatial attention. Behav. Brain Res. 237, 107–123.
Chica, A.B., Bartolomeo, P., Valero-Cabré, A., 2011. Dorsal and ventral parietal contributions to spatial orienting in the human brain. J. Neurosci. 31 (22), 8143–8149.
Chica, A.B., Valero-Cabré, A., Paz-Alonso, P.M., Bartolomeo, P., 2014. Causal contributions of the left frontal eye field to conscious perception. Cerebr. Cortex 24 (3), 745–753.
Cohen, J., 1977. In: rev (Ed.), Statistical Power Analysis for the Behavioral Sciences. Lawrence Erlbaum Associates, Inc, Hillsdale, NJ.
Correa, Á., Cona, G., Arbula, S., Vallesi, A., Bisiacchi, P., 2014. Neural dissociation of automatic and controlled temporal preparation by transcranial magnetic stimulation. Neuropsychologia 65, 131–136.
Correa, Á., Lupiáñez, J., Milliken, B., Tudela, P., 2004. Endogenous temporal orienting of attention in detection and discrimination tasks. Percept. Psychophys. 66 (2), 264–278.
Cotti, J., Rohenkohl, G., Stokes, M., Nobre, A.C., Coull, J.T., 2011. Functionally dissociating temporal and motor components of response preparation in left intraparietal sulcus. NeuroImage 54 (2), 1221–1230.
Coull, J.T., 2015. Directing attention in time as a function of temporal expectation. In: Toga, Arthur W. (Ed.), Brain Mapping: an Encyclopedic Reference, vol. 2. Academic Press: Elsevier, pp. 687–693.
Coull, J.T., Cotti, J., Vidal, F., 2016. Differential roles for parietal and frontal cortices in fixed versus evolving temporal expectations: dissociating prior from posterior temporal probabilities with fMRI. NeuroImage 141, 40–51.
Coull, J.T., Davranche, K., Nazarian, B., Vidal, F., 2013. Functional anatomy of timing differs for production versus prediction of time intervals. Neuropsychologia 51 (2), 309–319.
Coull, J.T., Nobre, A.C., 1998. Where and when to pay attention: the neural systems for directing attention to spatial locations and to time intervals as revealed by both PET and fMRI. J. Neurosci. 18, 7426–7435.

Coull, J.T., Nobre, A.C., Frith, C.D., 2001. The noradrenergic alpha 2 agonist clonidine modulates behavioural and neuroanatomical correlates of human attentional orienting and alerting. Cerebr. Cortex 11 (1), 73–84.
Coull, J.T., Vidal, F., Goulon, C., Nazarian, B., Craig, C., 2008. Using time-to-contact information to assess potential collision modulates both visual and temporal prediction networks. Front. Hum. Neurosci. 2, 10.
Davranche, K., Nazarian, B., Vidal, F., Coull, J., 2011. Orienting attention in time activates left intraparietal sulcus for both perceptual and motor task goals. J. Cognit. Neurosci. 23 (11), 3318–3330.
de Graaf, T.A., Sack, A.T., 2018. When and how to interpret null results in NIBS: a taxonomy based on prior expectations and experimental design. Front. Neurosci. 12, 915.
de Graaf, T.A., Sack, A.T., 2011. Null results in TMS: from absence of evidence to evidence of absence. Neurosci. Biobehav. Rev. 35 (3), 871–877.
Dell'Acqua, F., Scifo, P., Rizzo, G., Catani, M., Simmons, A., Scotti, G., et al., 2010. A modified damped Richardson-Lucy algorithm to reduce isotropic background effects in spherical deconvolution. NeuroImage 49 (2), 1446–1458.
Dell'Acqua, F., Simmons, A., Williams, S.C.R., Catani, M., 2013. Can spherical deconvolution provide more information than fiber orientations? Hindrance modulated orientational anisotropy, a true-tract specific index to characterize white matter diffusion. Hum. Brain Mapp. 34 (10), 2464–2483.
Doricchi, F., Thiebaut de Schotten, M., Tomaiuolo, F., Bartolomeo, P., 2008. White matter (dis)connections and gray matter (dys)functions in visual neglect: gaining insights into the brain networks of spatial awareness. Cortex 44 (8), 983e995.
Faul, F., Erdfelder, E., Lang, A.G., Buchner, A., 2007. G*Power 3: a flexible statistical power analysis program for the social, behavioral, and biomedical sciences. Behav. Res. Methods 39 (2), 175–191.
Fernández, A., Carrasco, M., 2020. Extinguishing exogenous attention via transcranial magnetic stimulation. Curr. Biol. 30 (20), 4078–4084 e3.
Gallotto, S., Schuhmann, T., Duecker, F., Middag-van Spanje, M., de Graaf, T.A., Sack, A. T., 2022. Concurrent frontal and parietal network TMS for modulating attention. iScience 25 (3), 103962.
Gomez-Tames, J., Hamasaka, A., Laakso, I., Hirata, A., Ugawa, Y., 2018. Atlas of optimal coil orientation and position for TMS: a computational study. Brain Stimul. 11 (4), 839–848.
Guo, F., Leemans, A., Viergever, M.A., Dell'Acqua, F., De Luca, A., 2020. Generalized Richardson-Lucy (GRL) for analyzing multi-shell diffusion MRI data. NeuroImage 218, 116948.
Herbst, S.K., Fiedler, L., Obleser, J., 2018. Tracking temporal hazard in the human electroencephalogram using a forward encoding model. eNeuro 5. ENEURO-0017.
Hilgetag, C.C., Théoret, H., Pascual-Leone, A., 2001. Enhanced visual spatial attention ipsilateral to rTMS-induced "virtual lesions" of human parietal cortex. Nat. Neurosci. 4, 953–957.
Irfanoglu, M.O., Walker, L., Sarlls, J., Marenco, S., Pierpaoli, C., 2012. Effects of image distortions originating from susceptibility variations and concomitant fields on diffusion MRI tractography results. NeuroImage 61 (1), 275–288.
Janssen, P., Shadlen, M.N., 2005. A representation of the hazard rate of elapsed time in macaque area LIP. Nat. Neurosci. 8, 234–241.
JASP Team, 2022. JASP. Version 0.16.1)[Computer software].
Jeurissen, B., Tournier, J.D., Dhollander, T., Connelly, A., Sijbers, J., 2014. Multi-tissue constrained spherical deconvolution for improved analysis of multi-shell diffusion MRI data. NeuroImage 103, 411–426.
Jung, J., Bungert, A., Bowtell, R., Jackson, S.R., 2016. Vertex stimulation as a control site for transcranial magnetic stimulation: a concurrent TMS/fMRI study. Brain Stimul. 9 (1), 58–64.
Keefe, J.M., Störmer, V.S., 2021. Lateralized alpha activity and slow potential shifts over visual cortex track the time course of both endogenous and exogenous orienting of attention. NeuroImage 225, 117495.
Kingstone, A., 1992. Combining expectancies. Q. J. Exp. Psychol. *44*A, 69–104.
Klarborg, B., Skak Madsen, K., Vestergaard, M., Skimminge, A., Jernigan, T.L., Baare, W. F.C., 2013. Sustained attention is associated with right superior longitudinal fasciculus and superior parietal white matter microstructure in children. Hum. Brain Mapp. 34 (12), 3216e3232.
Koch, G., Oliveri, M., Cheeran, B., Ruge, D., Lo Gerfo, E., Salerno, S., Torriero, S., Marconi, B., Mori, F., Driver, J., Rothwell, J.C., Caltagirone, C., 2008. Hyperexcitability of parietal-motor functional connections in the intact left-hemisphere of patients with neglect. Brain 131 (Pt 12), 3147–3155.
Kuhns, A.B., Dombert, P.L., Mengotti, P., Fink, G.R., Vossel, S., 2017. Spatial attention, motor intention, and bayesian cue predictability in the human brain. J. Neurosci. 37 (21), 5334–5344.
Laakso, I., Hirata, A., Ugawa, Y., 2014. Effects of coil orientation on the electric field induced by TMS over the hand motor area. Phys. Med. Biol. 59 (1), 203–218.
Leemans, A., Jeurissen, B., Sijbers, J., Jones, D.K., 2009. ExploreDTI: a graphical toolbox for processing, analyzing, and visualizing diffusion MR data. In: *17th Annual Meeting of the International Society Magnetic Resonance in Medicine*, p. 3537. Hawaii, USA.
Leemans, A., Jones, D.K., 2009. The B-matrix must be rotated when correcting for subject motion in DTI data. Magn. Reson. Med. 61 (6), 1336–1349.
Los, S.A., Kruijne, W., Meeter, M., 2014. Outlines of a multiple trace theory of temporal preparation. Front. Psychol. 5, 1058.
Maeda, F., Keenan, J.P., Tormos, J.M., Topka, H., Pascual-Leone, A., 2000. Modulation of corticospinal excitability by repetitive transcranial magnetic stimulation. Clin. Neurophysiol. 111, 800–805.
Martín-Arévalo, E., Lupiáñez, J., Narganes-Pineda, C., Marino, G., Colás, I., Chica, A.B., 2019. The causal role of the left parietal lobe in facilitation and inhibition of return. Cortex 117, 311–322.
Martín-Signes, M., Cano-Melle, C., Chica, A.B., 2021. Fronto-parietal networks underlie the interaction between executive control and conscious perception: evidence from TMS and DWI. Cortex 134, 1–15.
Martín-Signes, M., Pérez-Serrano, C., Chica, A.B., 2019. Causal contributions of the SMA to alertness and consciousness interactions. Cerebr. Cortex 29 (2), 648–656.
Mento, G., Tarantino, V., 2015. Developmental trajectories of internally and externally driven temporal prediction. PLoS One 10 (8), e0135098.
Miniussi, C., Wilding, E.L., Coull, J.T., Nobre, A.C., 1999. Orienting attention in time. Modulation of brain potentials. Brain 122, 1507–1518.
Muellbacher, W., Ziemann, U., Boroojerdi, B., Hallett, M., 2000. Effects of low-frequency transcranial magnetic stimulation on motor excitability and basic motor behavior. Clin. Neurophysiol. 111, 1002–1007.
Nakajima, R., Kinoshita, M., Shinohara, H., Nakada, M., 2019. The superior longitudinal fascicle: reconsidering the fronto-parietal neural network based on anatomy and function. Brain Imaging Behav. 14 (6), 2817–2830.
Niemi, P., Näätänen, R., 1981. Foreperiod and simple reaction time. Psychol. Bull. 89 (1), 133.
Nobre, A.C., 2010. How can temporal expectations bias perception and action. In: Coull, J.T., Nobre, A.C. (Eds.), Attention and Time. Oxford University Press, New York, pp. 371–392.
Nobre, A.C., van Ede, F., 2018. Anticipated moments: temporal structure in attention. Nat. Rev. Neurosci. 19 (1), 34–48.
Orpella, J., Ripollés, P., Ruzzoli, M., Amengual, J.L., Callejas, A., Martinez-Alvarez, A., et al., 2020. Integrating when and what information in the left parietal lobe allows language rule generalization. PLoS Biol. 18 (11), e3000895.
Ortiz-Tudela, J., Martín-Arévalo, E., Chica, A.B., Lupiáñez, J., 2018. Semantic incongruity attracts attention at a pre-conscious level: evidence from a TMS study. Cortex 102, 96–106.
Posner, M.I., 1980. Orienting of attention. Q. J. Exp. Psychol. 32, 3–25.
Rohenkohl, G., Gould, I.C., Pessoa, J., Nobre, A.C., 2014. Combining spatial and temporal expectations to improve visual perception. J. Vis. 14 (4), 1–13, 8.
Rojkova, K., Volle, E., Urbanski, M., Humbert, F., Dell'Acqua, F., Thiebaut de Schotten, M., 2016. Atlasing the frontal lobe connections and their variability due to age and education: a spherical deconvolution tractography study. Brain Struct. Funct. 221 (3), 1751–1766.
Rossi, S., Antal, A., Bestmann, S., Bikson, M., Brewer, C., Brockmöller, J., Carpenter, L.L., Cincotta, M., Chen, R., Daskalakis, J.D., Di Lazzaro, V., Fox, M.D., George, M.S., Gilbert, D., Kimiskidis, V.K., Koch, G., Ilmoniemi, R.J., Lefaucheur, J.P., Leocani, L., Lisanby, S.H., et al., 2021. Safety and recommendations for TMS use in healthy subjects and patient populations, with updates on training, ethical and regulatory issues: expert Guidelines. Clin. Neurophysiol. 132 (1), 269–306.
Rossini, P.M., Burke, D., Chen, R., Cohen, L.G., Daskalakis, Z., Di Iorio, R., Di Lazzaro, V., Ferreri, F., Fitzgerald, P.B., George, M.S., Hallett, M., Lefaucheur, J.P., Langguth, B., Matsumoto, H., Miniussi, C., Nitsche, M.A., Pascual-Leone, A., Paulus, W., Rossi, S., Rothwell, J.C., Ziemann, U., 2015. Non-invasive electrical and magnetic stimulation of the brain, spinal cord, roots and peripheral nerves: basic principles and procedures for routine clinical and research application. An updated report from an I.F.C.N. Committee. Clin. Neurophysiol. 126 (6), 1071–1107.
Sasson, E., Doniger, G.M., Pasternak, O., Tarrasch, R., Assaf, Y., 2012. Structural correlates of cognitive domains in normal aging with diffusion tensor imaging. Brain Struct. Funct. 217 (2), 503e515.
Sasson, E., Doniger, G.M., Pasternak, O., Tarrasch, R., Assaf, Y., 2013. White matter correlates of cognitive domains in normal aging with diffusion tensor imaging. Fla. Nurse 7, 32.
Schneider, W., Eschman, A., Zuccolotto, A., 2002. E-Prime: User's Guide. Reference Guide. *Getting Started Guide*. Psychology Software Tools, Incorporated.
Smith, D.T., Jackson, S.R., Rorden, C., 2005. Transcranial magnetic stimulation of the left human frontal eye fields eliminates the cost of invalid endogenous cues. Neuropsychologia 43 (9), 1288–1296.
Thiebaut de Schotten, M., Ffytche, D.H., Bizzi, A., Dell'Acqua, F., Allin, M., Walshe, M., Murray, R., Williams, S.C., Murphy, D.G., Catani, M., 2011. Atlasing location, asymmetry and inter-subject variability of white matter tracts in the human brain with MR diffusion tractography. NeuroImage 54 (1), 49–59.
Thiebaut de Schotten, M., Tomaiuolo, F., Aiello, M., Merola, S., Silvetti, M., Lecce, F., et al., 2014. Damage to white matter pathways in subacute and chronic spatial neglect: a group study and 2 single-case studies with complete virtual "in vivo" tractography dissection. Cerebr. Cortex 24 (3), 691e706.
Triviño, M., Arnedo, M., Lupiánez, J., Chirivella, J., Correa, Á., 2011. Rhythms can overcome temporal orienting deficit after right frontal damage. Neuropsychologia 49 (14), 3917–3930.
Triviño, M., Correa, A., Arnedo, M., Lupiáñez, J., 2010. Temporal orienting deficit after prefrontal damage. Brain 133 (4), 1173–1185.
Triviño, M., Correa, Á., Lupiáñez, J., Funes, M.J., Catena, A., He, X., Humphreys, G.W., 2016. Brain networks of temporal preparation: a multiple regression analysis of neuropsychological data. NeuroImage 142, 489–497.
Vallesi, A., Lozano, V.N., Correa, A., 2013. Dissociating temporal preparation processes as a function of the inter-trial interval duration. Cognition 127 (1), 22–30.
Vallesi, A., Visalli, A., Gracia-Tabuenca, Z., Tarantino, V., Capizzi, M., Alcauter, S., Mantini, D., Pini, L., 2022. Fronto-parietal homotopy in resting-state functional connectivity predicts task-switching performance. Brain Struct. Funct. 227 (2), 655–672.
Visalli, A., Capizzi, M., Ambrosini, E., Kopp, B., Vallesi, A., 2021. Electroencephalographic correlates of temporal Bayesian belief updating and surprise. NeuroImage 231, 117867.
Visalli, A., Capizzi, M., Ambrosini, E., Mazzonetto, I., Vallesi, A., 2019. Bayesian modeling of temporal expectations in the human brain. NeuroImage 202, 116097.

Wagenmakers, E.J., Marsman, M., Jamil, T., Ly, A., Verhagen, J., Love, J., Selker, R., Gronau, Q.F., Šmíra, M., Epskamp, S., Matzke, D., Rouder, J.N., Morey, R.D., 2018. Bayesian inference for psychology. Part I: theoretical advantages and practical ramifications. Psychonomic Bull. Rev. 25 (1), 35–57.

Wagner, T., Valero-Cabre, A., Pascual-Leone, A., 2007. Noninvasive human brain stimulation. Annu. Rev. Biomed. Eng. 9, 527–565.

Wang, R., Benner, T., Sorensen, A.G., Wedeen, V.J., 2007. Diffusion toolkit: a software package for diffusion imaging data processing and tractography. Proc. Int. Society Magn. Resonance. Med. 15, 3720.

Wolfers, T., Onnink, A.M.H., Zwiers, M.P., Arias-Vasquez, A., Hoogman, M., Mostert, J. C., et al., 2015. Lower white matter microstructure in the superior longitudinal fasciculus is associated with increased response time variability in adults with attention-deficit/hyperactivity disorder. J. Psychiatry Neurosci. 40 (5), 344e351.

Xia, M., Wang, J., He, Y., 2013. BrainNet Viewer: a network visualization tool for human brain connectomics. PLoS One 8 (7), e68910.

Yeshurun, Y., Tkacz-Domb, S., 2021. The time-course of endogenous temporal attention -Super fast voluntary allocation of attention. Cognition 206, 104506.

Zlatkina, V., Petrides, M., 2014. Morphological patterns of the intraparietal sulcus and the anterior intermediate parietal sulcus of Jensen in the human brain. Proc. Biol. Sci. 281 (1797), 20141493.